JOURNAL OF MATERIALS SCIENCE 17 (1982) 769–778

Room temperature strengthening mechanisms in a Co-Cr-Mo-C alloy

KRISHNA RAJAN
National Aeronautical Establishment, National Research Council, Ottawa, Ontario, K1A 0R6, Canada

JOHN B. VANDER SANDE
Department of Materials Science and Engineering, Massachusetts Institute of Technology, Cambridge, MA. 02139, USA

The various contributions to the flow stress at room temperature of a cast Co–Cr–Mo–C alloy were identified using transmission electron microscopy. These alloys are used as surgical implant materials. It was concluded that stacking fault intersections and twins make the largest contribution to the work hardening behaviour of the as-cast Co–Cr–Mo–C alloy. The stacking fault intersection was modelled as a form of dislocation dipole, from which the stress interaction with slip dislocations was estimated. In the case of twin-slip interactions, it is suggested that the incorporation of the slip dislocation into the twin is governed by the reaction

$$\tfrac{1}{2}[1\,1\,0]_{(\bar{1}\,1\,\bar{1})} \rightarrow \tfrac{1}{6}[1\,4\,1]_{(\bar{1}\,\bar{1}\,5)} + \tfrac{1}{6}[2\,\bar{1}\,\bar{1}]_{\substack{\text{Coherent Twin}\\ \text{Boundary (1 1 1)}}}$$

A nucleation model for twinning in alloys with very low stacking fault energy is also proposed.

1. Introduction

Investment castings of Co–Cr–Mo–C alloys (known commercially as Vitallium or HS.21) are widely used as surgical implants. Unfortunately, despite the extensive use of these alloys as surgical implant materials, the shortcomings of these alloy systems are evident in the mechanical failure statistics of weight bearing prostheses [1]. This provides a disturbing commentary on the extent of knowledge of the metallurgical characteristics of these complex cobalt-based alloys. Despite the attention given to the alloy system as surgical implant material [2–6], there is still a need for a basic understanding of the structure–property relationships in these cobalt-based alloys. Specifically, the primary purpose of the study was to determine, using transmission electron microscopy, the various contributions to the flow stress at room temperature of a cast Co–Cr–Mo–C alloy.

The material used for surgical implants falls into the category of superalloys as the composition of this alloy (Table I) is similar to conventional cobalt-based superalloys [7]. While the high temperature mechanical behaviour of cobalt alloys is well documented [8–10], the room temperature behaviour has not been studied extensively [11]. The work described here focused on as-cast Vitallium, as most of the material in service as surgical implants today is used in the as-cast condition.

TABLE I Composition of as-cast alloy used in the present study

Element	Content (wt %)
Cr	28.5
Mo	5.7
Ni	2.2
Fe	0.4
C	0.3
Si	0.4
Mn	0.5
Co	Balance

0022–2461/82/030769–10$03.70/0

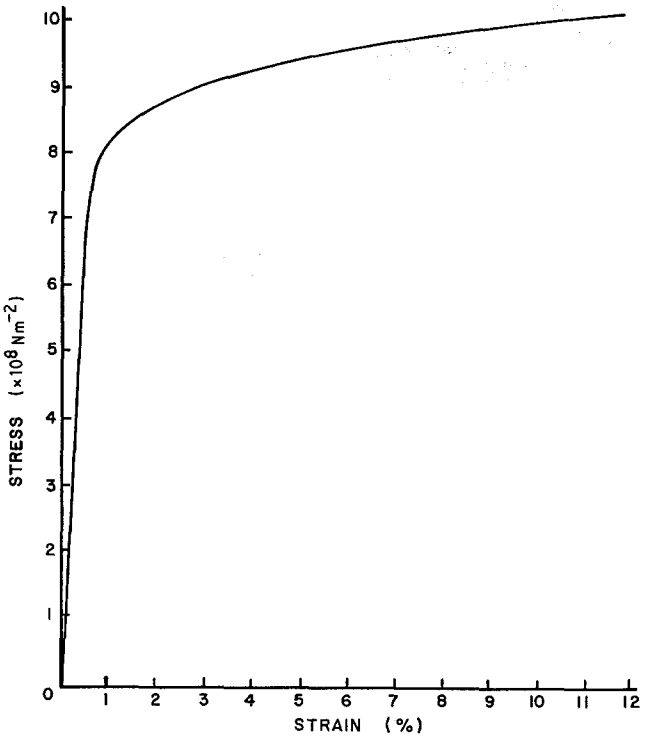

Figure 1 Stress–strain curve for as-cast Co–Cr–Mo–C alloy.

2. Experimental details

The samples were cast into the form of cylindrical tensile samples. Specimens were deformed in tension and the deformation was interrupted at various stages of the stress–strain curve. The dislocation structure in these samples was observed by transmission electron microscopy. The microscopy was performed using disc-shaped specimens, 3 mm in diameter. The discs were sliced from the gauge length of the tensile sample using a spark cutter, to a thickness of 0.3 mm. The samples were finally thinned using conventional jet polishing techniques in a solution of methanol–15 vol% sulphuric acid, operating at -50° C and 0.5 A cm^{-2} current density.

3. Experimental results

Four states of tensile deformation were examined by electron microscopy; the undeformed condition, 4% engineering strain, 7% strain, and 11% strain at fracture (see Fig. 1).

There were a number of dislocations, probably intrinsic to the as-received state. All the dislocations, however, were dissociated into their respective partials. Thus the structure was characterized by the presence of stacking faults (see Fig. 2). On any given plane, the stacking fault width, while large, was not constant. In many of the stacking faults, the partial dislocations were not parallel, as in an infinite medium, but bound the stacking fault trapezoidally. As discussed in detail by Kroner *et al.* [12], this effect is due to the fact that each of the partials has a different Burgers vector and therefore tends to intersect the surface at a different angle. This leads to constriction at one end and to extension on the other foil surface.

Even with careful handling of the thin foils, with a slight amount of stress, the stacking faults expand to extremely large widths. This gives rise to the long bands of stacking faults as shown in Fig. 3.

The stacking faults formed by deformation were intrinsic faults on {1 1 1} planes of the fcc matrix as shown by the contrast experiment of Fig. 4. This contrast experiment, as suggested by Gevers *et al.* [13], is based on the fact that in dark-field, the operating reflection, **g**, points away from the light fringe, when the **g** vector is centred on the fault, if the fault is intrinsic. The **g** vector points toward the light fringe if the fault is extrinsic. The reflections to be used are {1 1 1}, {2 2 0} and {4 4 0}. The opposite rule applies for {2 0 0}, {2 2 2} and {4 4 0}. This contrast experiment is independent of the inclination of the fault. Thus Fig. 4 proves that the fault is intrinsic. In carrying

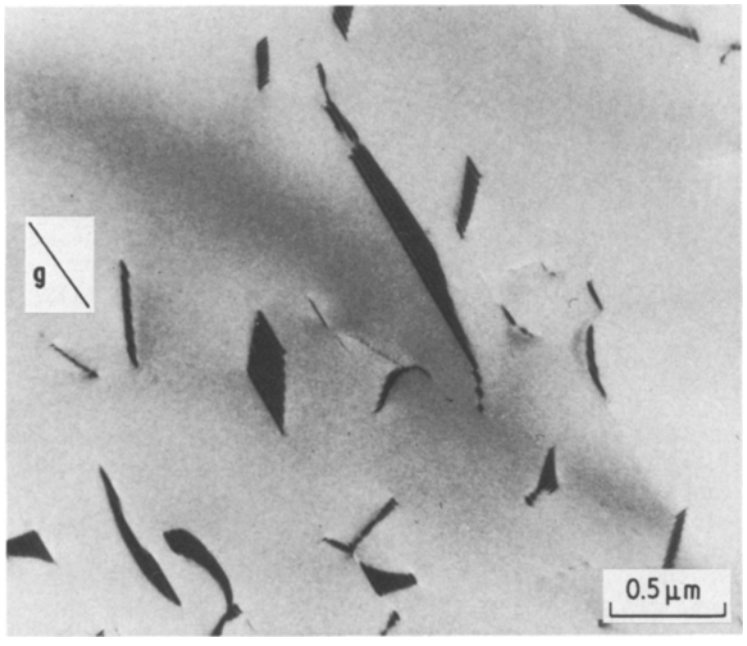

Figure 2 Microstructure of undeformed material, showing dissociated dislocations, $\mathbf{g} = [1\bar{1}1]$.

out this type of experiment it is important to avoid overlapping stacking faults and to use single faults only.

The microstructure, shown in Fig. 5, is characteristic of the early stages of plastic deformation. The stacking fault density has increased from the undeformed state. This has resulted in the formation of a number of stacking fault intersections. There is also evidence of overlapping stacking faults. Fig. 5b was obtained using $\mathbf{g} = \{2\,2\,0\}$ thus producing dislocation contrast and making the stacking faults invisible. Besides delineating the partial dislocations from the stacking faults there appears to be a high dislocation density within the confines of the stacking faults.

To examine the specific nature of these dislocations, a Burgers vector, **b**, analysis was carried out on one such set of dislocations. In performing

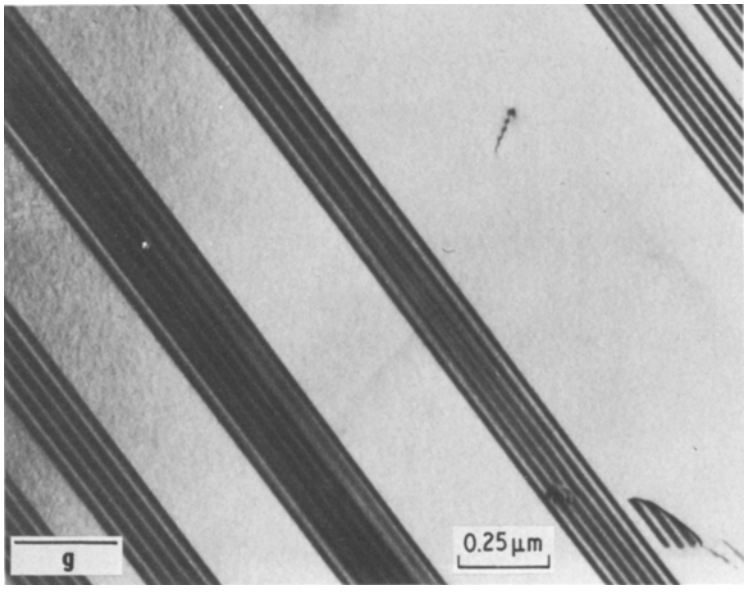

Figure 3 Representative view of stacking fault bands, $\mathbf{g} = [2\,0\,0]$.

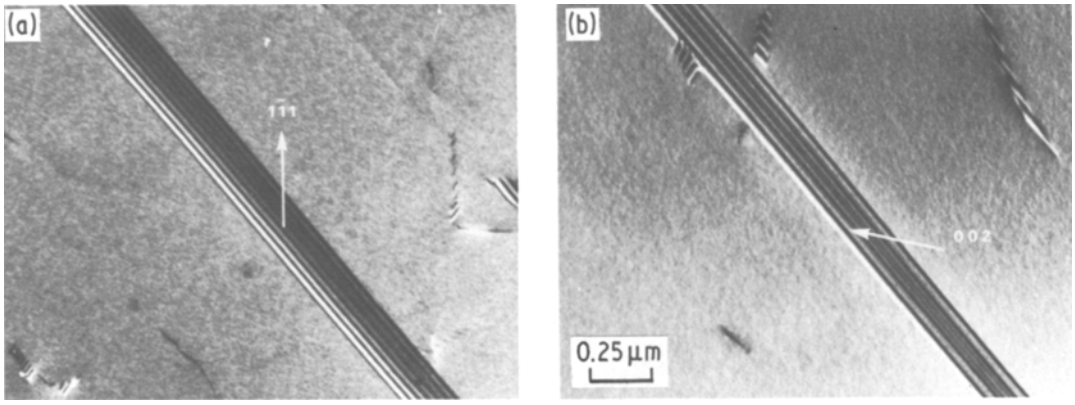

Figure 4 Dark-field images illustrating intrinsic nature of stacking faults, with (a) $\mathbf{g} = \langle 1\,1\,1 \rangle$ pointing away from the light fringe and (b) $\mathbf{g} = \langle 0\,0\,2 \rangle$ pointing toward it.

such an analysis, both Shockley partial dislocations and perfect dislocations have to be considered at the same time. Using two-beam diffraction conditions, the $\mathbf{g} \cdot \mathbf{b} = 0$ rule for invisibility or weak contrast for perfect dislocations was applied. Partial dislocations, however, are invisible or have weak contrast for $\mathbf{g} \cdot \mathbf{b}_p = 0$ and $\pm 1/3$, (where the subscript p refers to partial) for small deviation parameters [14]. Due to the problems associated with $\mathbf{g} \cdot \mathbf{b}_p = \pm 2/3$ those reflections giving such values for $\mathbf{g} \cdot \mathbf{b}$ were not used for unambiguous determination of the Burgers vector [15, 16].

Let us now consider a set of dislocations residing within the confines of a stacking fault as shown in Fig. 6a and drawn schematically in Fig. 6b.

Dislocations 1 to 7 and 9 (Group 1) were determined to have a Burgers vector $\mathbf{b}_{\text{Group 1}} = 1/2\,[1\,0\,\bar{1}]$. If $\mathbf{b} = 1/6\,[1\,\bar{2}\,1]$, then the dislocations should be invisible or have weak contrast for $\mathbf{g} = [\bar{1}\,1\,3]$ and $\mathbf{g} = [0\,0\,2]$ since $\mathbf{g} \cdot \mathbf{b}_p = 0$ and $1/3$ respectively. However they were visible, thus $\mathbf{b} \neq 1/6\,[1\,\bar{2}\,1]$. Also they were visible for $\mathbf{g} = [1\,\bar{1}\,\bar{1}]$ ruling out $\mathbf{b} = 1/6\,[1\,1\,\bar{2}]$ and $\mathbf{b} = 1/6\,[\bar{2}\,1\,1]$ for which $\mathbf{g} \cdot \mathbf{b}_p = 1/3$ and 0 respectively.

Dislocations 6A, 7A and 9A, forming Group 2, seem to be connecting or junction type dislocations branching from the perfect dislocations. They were invisible for $\mathbf{g} = [\bar{1}\,1\,\bar{1}]$ and $\mathbf{g} = [1\,\bar{1}\,\bar{1}]$ thus ruling out $\mathbf{b} = 1/2\langle 1\,1\,0 \rangle$. They were visible for $\mathbf{g} = [1\,\bar{1}\,3]$ eliminating $\mathbf{b} = 1/6\,[\bar{2}\,1\,1]$ and visible for $\mathbf{g} = [2\,\bar{2}\,0]$ ruling out $\mathbf{b} = 1/6\,[1\,1\,\bar{2}]$ as $\mathbf{g} \cdot \mathbf{b}_p = 0$ for both these cases. Thus $\mathbf{b}_{\text{Group 2}} = 1/6\,[1\,\bar{2}\,1]$.

Similarly, Dislocations 8, 10, 11 and 13, which constitute Group 3, were found to have a Burgers vector of $\mathbf{b}_{\text{Group 3}} = 1/6\,[\bar{2}\,1\,1]$.

The presence of slip dislocations on stacking faults carries with it important implications in terms of work hardening. As shown in Fig. 7, these

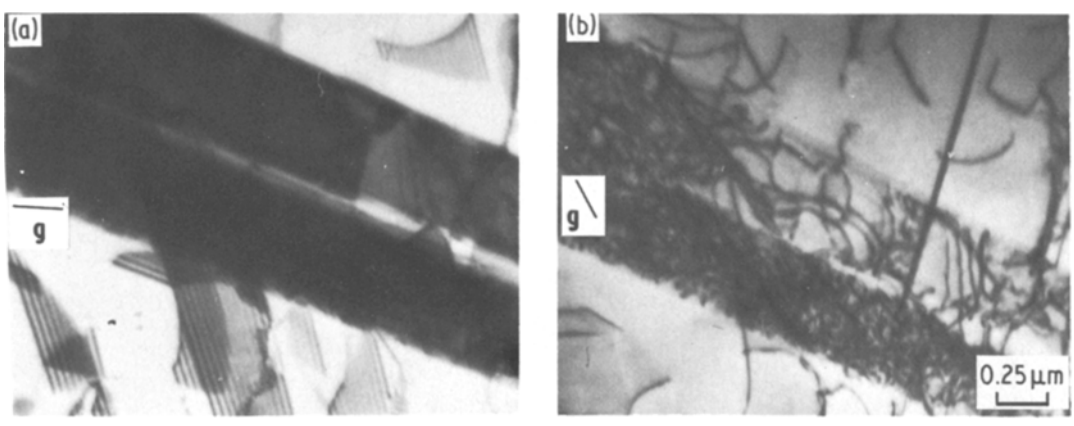

Figure 5 Typical microstructure of sample deformed by 4%, showing high dislocation density within confines of the stacking faults.

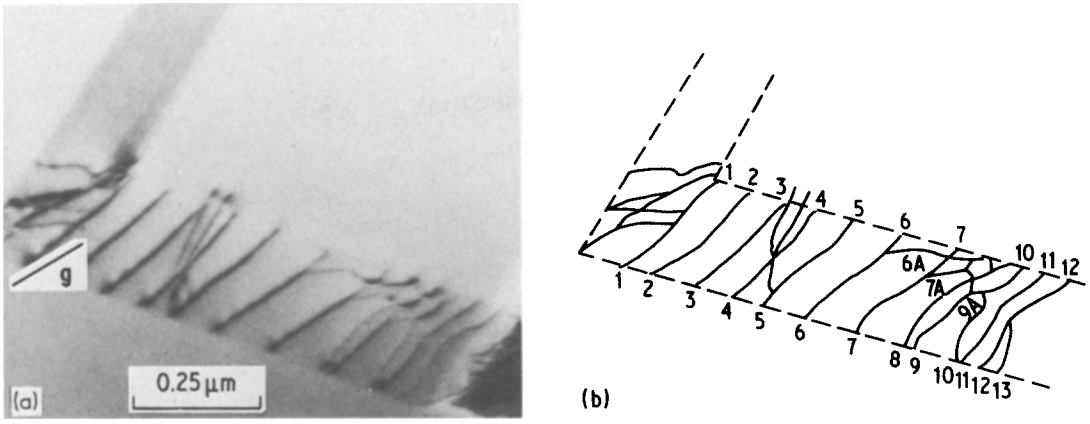

Figure 6 (a) A detailed view, $g = [2\bar{2}0]$ (b) schematic diagram of dislocation array in a stacking fault. See text for identification of each group of dislocations.

dislocations encounter stacking fault intersections and pile-up at the intersections. This would suggest that stacking fault intersections are a major obstacle to dislocation motion. An analysis of this point will be made later in the discussion.

The deformation substructure with 7% strain, exhibited a greater density of intersecting and overlapping bands of stacking faults. Again, the stacking faults seem to be regions of intense localized deformation.

At fracture, the stacking fault and stacking fault intersection density was much more abundant. Another feature that was more evident was the presence of twins. It should be noted that the distinction between an fcc twin and a hcp platelet can be made using electron diffraction. Following the treatment of Kestenbach [17], an unambiguous analysis of the structure can be made when the electron diffraction patterns are observed in certain orientations. For example, the $[1\bar{1}0]$ beam direction in the fcc matrix provides for the extra spots from twins to be distinct from those of hcp plates on (1 1 1) matrix planes (see Fig. 8). A number of observations were made using this technique and it was found that fcc twins, not hcp, dominated the microstructure. This analysis was carried out at all strains. Twins are prominent throughout the deformation process which would suggest that they contribute strongly to strain hardening.

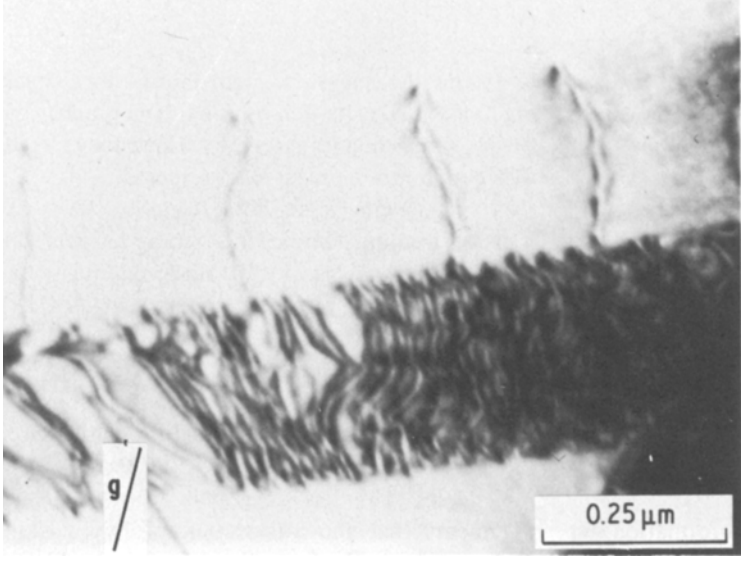

Figure 7 Dislocation pile-ups at stacking fault intersections, $g = [0\,2\,2]$.

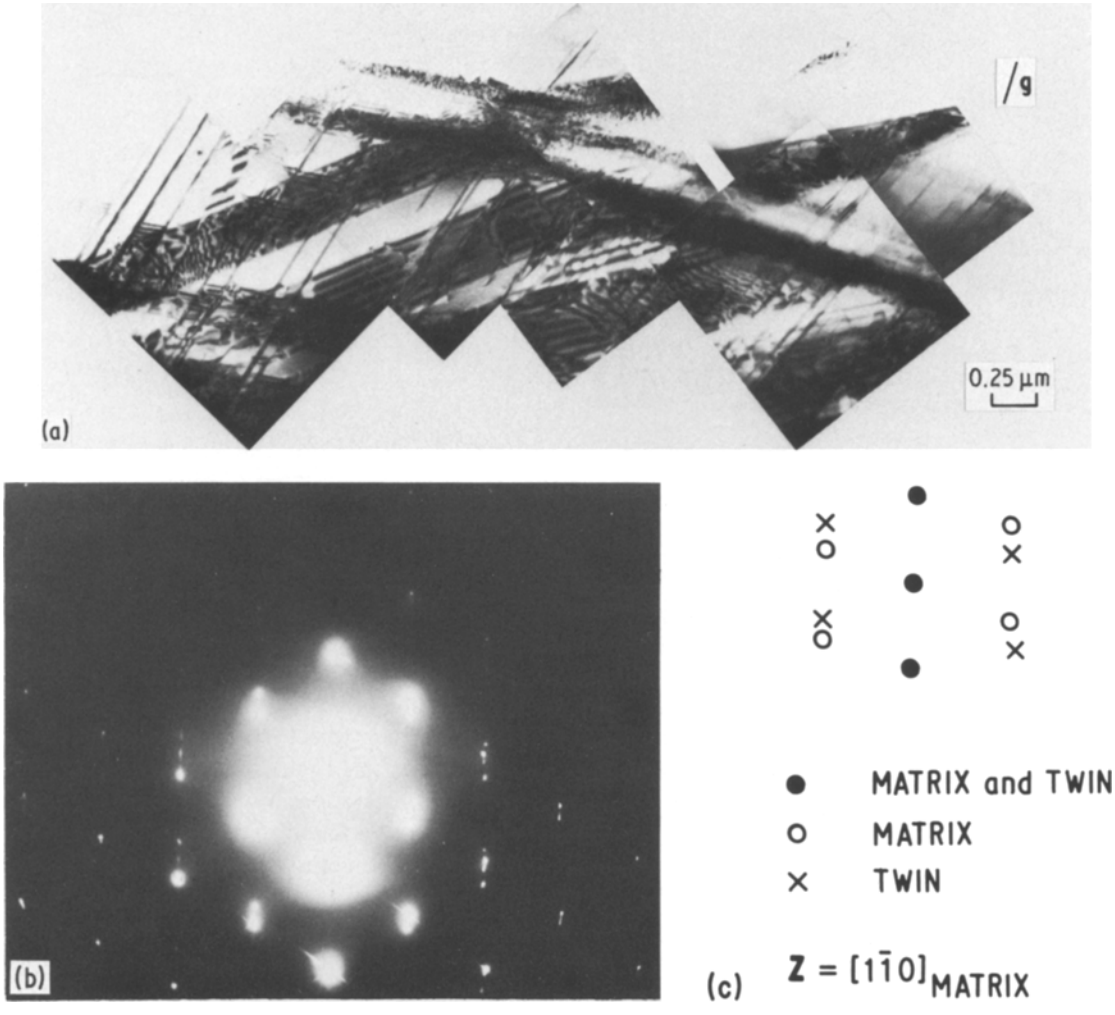

Figure 8 (a) A typical microstructure, $\mathbf{g} = [0\,0\,\bar{2}]$; (b) a diffraction pattern with (c) an interpretation of a region with a high twin density. In ⟨1 1 0⟩ matrix orientation, the twin spots can be distinguished from h c p spots, which were not present here.

4. Discussion

From observations of the deformation microstructure of this as-cast Co-based alloy, it is found that the two primary features are the presence of stacking faults and twins. In the following discussion, the mechanisms by which stacking faults and twins contribute to the flow stress of the alloy are presented. Also, in the course of examining twinning, the need for a new nucleation model of twinning is discussed and its mechanism is proposed.

4.1. The role of stacking faults in strengthening

The primary characteristic of the deformation substructure is the presence of wide stacking faults and twins. To analyse the contribution these stacking faults make to the work-hardening behaviour of this alloy, the mechanism by which they impede dislocation motion must be considered.

While stacking faults do act as obstacles to dislocation motion, they are not strong barriers. The high number of successful stacking fault intersections observed attests to this (see Fig. 9) [18]. However, once this intersection is produced, this can prove to be a formidable obstacle to any further dislocation motion (see Fig. 7). Thus it is important to understand the nature of this intersection.

Ashbee [19] has suggested from geometric arguments that the intersection of two stacking faults results in the formation of a volume dilation

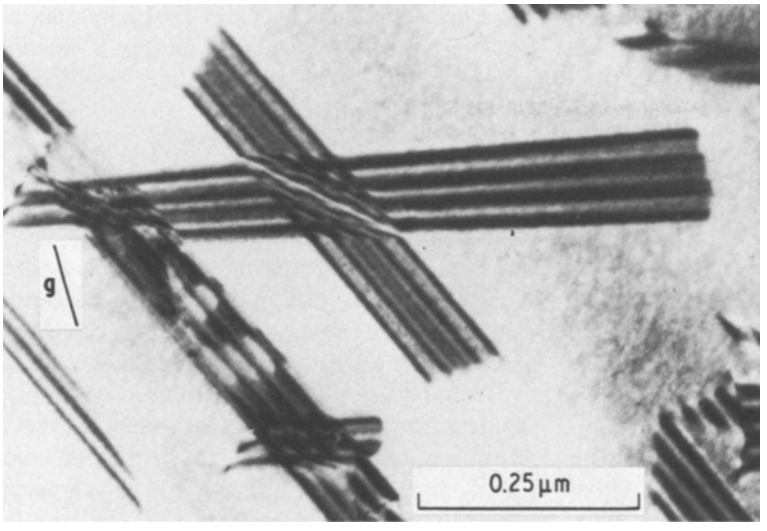

Figure 9 Stacking fault intersection, $\mathbf{g} = [1\bar{1}1]$.

along the line of intersection, which is equivalent to a row of vacancies. Thus it is worthwhile to consider the stacking fault intersection as a dislocation dipole. Since it has been shown in this work that stacking faults act as regions of localized slip it becomes very important to consider the nature of the interaction between slip dislocations and the dipole existing at this interesection of stacking faults. Dipoles have a stress field which tends to zero with $1/r^2$, where r is the distance from the dipole. Thus it is necessary to consider the interaction between a dislocation and a dipole only at very small distances (5**b** or less). At this stage, one is considering the interaction of dislocation cores. Thus the dislocation intersecting the dipole experiences the interaction force between the dipole dislocations themselves. In order to pass through this dipole, the intersecting dislocation must overcome the attractive force between the dipole dislocations. The maximum attractive force per unit length, F, between the dipole dislocations when separated by a distance y is given as [20]

$$F = \frac{-\mu \mathbf{b}^2}{8\pi(1-\nu)y}, \qquad (1)$$

where μ is the shear modulus and ν is Poisson's ratio. Following the treatment of Ashbee, the row of vacancies at the stacking fault intersection is actually a partial dislocation dipole. Thus, for our purpose, **b** in the above equation refers to a partial dislocation in the f c c lattice. The dipole separation, y, may also be estimated by using Ashbee's geometric argument. The volume dilation produced by the intersection is $a^3/18$, then y may be taken as $(a^3/18)^{1/3}$. The interactive force is thus approximately $0.26\,\mathrm{Nm}^{-1}$. The corresponding stress needed to separate the dipole dislocations, τ, is given by

$$\tau \simeq \frac{F}{|\mathbf{b}|} \simeq 2 \times 10^9\ \mathrm{Nm}^{-2}. \qquad (2)$$

This would be indicative of the stress needed for a perfect dislocation to pass through a stacking fault intersection (i.e. a dipole). The point of these calculations is simply to emphasize that stacking fault intersections, when treated as dislocation dipoles, can prove to be major obstacles for the motion of slip dislocations. Thus it is the stacking fault intersections and not stacking faults themselves which are the major impediments to dislocation motion.

4.2. Twinning

Before considering how twins contribute to the flow stress, the nucleation and growth of the twins must first be examined. In making such an examination, it was found that the existing nucleation models could not be satisfactorily applied to the present alloy system.

Recall that the formation of intrinsic stacking faults on every plane produces a twin in a f c c crystal. The problem of establishing a nucleation model comes in suggesting a process which will allow for the generation of a partial dislocation of just the right sign on each successive $\{1\,1\,1\}$ plane or the transfer of one partial from one plane to the next. Various models have been proposed which involve some form of a pole dislocation

[21–24]. The shortcoming of these mechanisms is that the pole dislocations, being glissile, will not be anchored strongly enough to prevent them from moving under the stress causing the sweeping dislocation to move. Other models involve the interaction of partials [25, 26]. However, with the large separation of partials present in this system, such an interaction is doubtful.

It was therefore necessary to consider an alternative mechanism of twin formation and growth consistent with the electron microscopy observations. The mechanism to be proposed here is based on a nucleation model by Olson and Cohen [20, 27] for the fcc → hcp martensitic transformation, which may be extended to consider twin nucleation as well.

4.2.1. Twin nucleation model

An important aspect of the Olson–Cohen (O–C) mechanism is the formation of a martensitic embryo by a faulting process derived from a group of already existing dislocations which happen to be appropriately spaced. The criterion used in this model for embryo formation in martensitic nucleation can also be used in the present study to explain twin nucleation. O–C suggest that the critical condition for the spontaneous formation of an embryo occurs when the fault energy is close to zero. The very low stacking fault energy in the present alloy system lends some physical support to the concept of a twin embryo, as the probability of the formation of a twin nucleus increases as the fault energy decreases.

O–C have used a pole mechanism to explain the growth of this embryo. However, as mentioned earlier, the presence of such a pole dislocation, which would be sessile on the plane of the transformation dislocation, was not evident. For example, Frank partials, which would have a screw component normal to the fault plane were never found. However, there are faults inclined to the fault plane containing the embryo. What we are suggesting is that stacking faults may provide the pole dislocations needed for the embryo to grow. Thus when the twin embryo intersects a stacking fault lying on a different plane, it effectively encounters two pole dislocations which are the two partials bounding the stacking fault.

In the limit, if a single transformation dislocation, $1/6\langle 1\,1\,2\rangle$, intersects these two pole dislocations, this is the equivalent to the intersection of two stacking faults. As Ashbee [19] and Heidenreich and Shockley [28] have pointed out, such an intersection produces a volume dilation in the lattice which Ashbee describes as a "partial dislocation doublet". This is analogous to the dipole formation suggested by O–C.

If a twin embryo intersects the stacking fault instead, a "partial doublet" is formed on each plane and the resulting doublet or dipole interaction is now much weaker for the same reasons as suggested in the O–C model. This would mean that the transformation dislocations can spiral around the stacking fault, moving onto consecutive close-packed planes with each revolution (see Fig. 10). The idea of dislocations wrapping themselves around a stacking fault may seem more acceptable if it is kept in mind that what is essentially operating is a "dissociated pole" mechanism, where for the embryo growth to occur, the transformation dislocation must intersect two partial dislocations, instead of a single perfect dislocation as in O–C case.

The stress necessary for twin nucleation from such a defect is given as [29]

$$\tau = \frac{2\sigma}{n\rho V s}, \tag{3}$$

where σ is the coherent twin boundary energy, n is the number of dislocations in embryo, ρ is the number of moles per unit area of close-packed plane, V is the molar volume, and s is the twinning shear. With the substitution of the appropriate values [18], the critical resolved shear stress necessary for twin nucleation is $4.5 \times 10^7\ \mathrm{Nm^{-2}}$. The yield stress for this alloy is approximately $8 \times 10^8\ \mathrm{Nm^{-2}}$. The shear stress is approximately one half of this. Thus the available stress at yield would be high enough to nucleate twins by this embryo mechanism.

4.2.2. Twin-slip interaction

In order to pass a dislocation through a twinned crystal, interface dislocations must in general be produced. This generation requires energy and this in turn must raise the applied shear stress for dislocation motion. It can, therefore be inferred that the finer the distribution of twins, the greater will be the density of interface dislocations and thus the higher the shear stress required for dislocation motion [30]. The generation of interface dislocations involves dissociations which are energetically unfavourable. The incorporation of slip dislocations with twins can occur

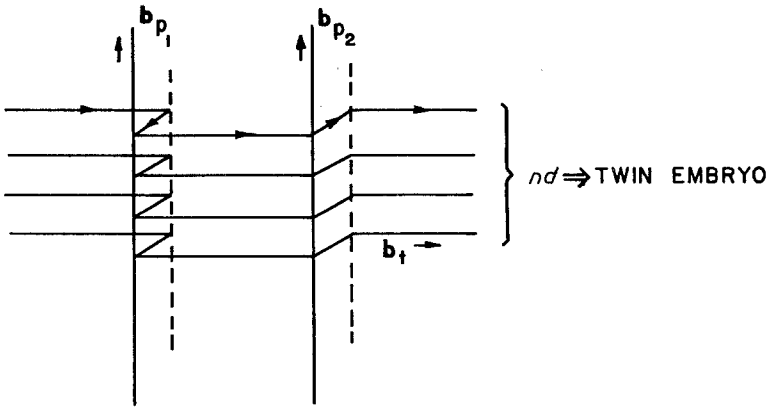

Figure 10 Schematic representation of embryo thickening by the dissociated pole mechanism.

when the applied stress is locally magnified, as in the presence of a dislocation pile-up. The types of dislocations that can occur at the coherent twin boundary (CTB) have been discussed in detail in the literature [31–33].

Unfortunately in this study, due to the high dislocation density, it was not possible to clearly identify the interfacial dislocations at the twin boundary. However, a number of dislocation pile-ups were observed with 20 to 25 dislocations. The externally applied shear stress which stabilizes such a pile-up is given by:

$$\tau_A = \frac{n\mu b}{\pi L}, \qquad (4)$$

where n is the number of dislocations in pile-up and L is the length of pile-up. A dislocation reaction suggested by a number of workers is [34–36]

$$1/2[1\,1\,0]_{(\bar{1}\,1\,1)} \rightarrow 1/6[1\,4\,1]_{(\bar{1}\,\bar{1}\,5)} + 1/6[2\,\bar{1}\,\bar{1}]_{CTB}.$$

If the stress needed for this energetically unfavourable reaction to occur is given by τ, then the minimum number of pile-up dislocations is governed by the condition $\tau = \tau_A$. Based on such calculations, the details of which are described elsewhere [18], it was found that at least ten dislocations in a pile-up were needed to indicate the presence of a stress concentration high enough to make the above dislocation reaction proceed. The fact that the calculated and experimentally observed values are of the same order of magnitude, show that this incorporation mechanism may in fact be operative at the twin–matrix interface.

The possible effects of other strengthening mechanisms including solid solution effects and dislocation stress field interactions were also considered. These, however, were found to provide a relatively small contribution to the flow stress [18]. Stacking fault intersections and twins provide the major obstacles to dislocation motion.

5. Conclusions

While the fcc→hcp transformation has always been considered important to the mechanical behaviour of cobalt-based alloys, its role has never been stated explicitly. The electron microscopy performed in this study has defined in specific terms the contributions of the fcc→hcp transition to the room temperature work-hardening behaviour of a cobalt-based alloy. Stacking fault formation and twin formation may be considered, from a structural standpoint, as precursors to hcp formation. The mechanism by which stacking faults and twins contribute to the flow stress was shown in this study. Localization of slip along stacking faults and the presence of dislocation pile-ups at stacking fault intersections and twins are examples of the role stacking faults and twins play in deformation.

The occurrence of fcc twinning as opposed to hcp formation carries with it an important implication. Both twins and hcp platelets can act as major obstacles to slip. In the hcp structure there is only one primary slip system, and thus ductility is severely limited, compared to the fcc structure. Thus fcc twinning provides a means of obtaining strength without sacrificing ductility in cobalt based alloys.

Due to the importance of stacking faults and twins, it follows that the stacking fault energy is a crucial parameter to consider. The lower the fault energy, the higher is the fault density and the higher is the twin density. An increase in the twin density would contribute to an

increase in the flow stress of the alloy. This in fact has been observed for the Co–Ni system at temperatures where twinning plays an important role in deformation [30].

Thus the results of the present study provide a microstructural basis for surgical implant alloy design and processing. In order to provide for an increase in flow stress with enhanced ductility, alloy composition and/or processing parameters must be selected so that plastic deformation proceeds predominantly by stacking fault formation and twinning.

Acknowledgements

The authors wish to thank Drs R. L. Hewitt and W. Wallace for many valuable discussions.

References

1. J. T. SCALES, *J. Bone Jt. Surg.* **53B** (1972) 344.
2. D. J. ARROWSMITH, *J. Sheffield Univ. Metall. Soc.* **6** (1967) 42.
3. J. L. KATZ, in "Biomaterials – Bioengineering Applied to Materials for Hard and Soft Tissue Replacements", edited by A. L. Bement Jr. (University of Washington Press, Seattle, 1971) p. 79.
4. H. L. MILLER, W. ROSTOKER and J. O. GALANTE, *J. Biomed. Mater. Res.* **10** (1976) 399.
5. E. SMETHURST and R. B. WATERHOUSE, *J. Mater. Sci.* **12** (1977) 1781.
6. E. KOROSTOFF (ED.) "Research in Dental and Medical Materials" (Plenum Press, New York, 1969).
7. C. P. SULLIVAN, M. J. DONACHIE Jr. and F. R. MORRAL, "Cobalt–Base Superalloys–1970" (Centre d'Information, Brussels, 1970).
8. C. T. SIMS, "The Superalloys", edited by C. T. Sims and W. C. Hagel (John Wiley and Sons, New York, 1972) p. 145.
9. N. J. GRANT, *ASM Trans.* **40** (1948) 585.
10. J. R. LANE and N. J. GRANT, *ibid.* **44** (1952) 113.
11. J. B. VANDER SANDE, J. R. COKE and J. WULFF, *Met. Trans. A* **7A** (1976) 389.
12. A. KORNER, H. P. KARNTHALER and H. O. K. KIRCHNER, *Phys. Stat. Sol.* **81** (1977) 1917.
13. R. GEVERS, A. ART and S. AMELINCKX, *ibid.* **B** (1963) 1563.
14. P. B. HIRSCH, A. HOWIE, R. B. NICHOLSON, D. W. PASHLEY and J. J. WHELAN, "Electron Microscopy of Thin Crystals" (Butterworths, London, 1965) p. 182.
15. J. M. SILCOCK and W. J. TUNSTALL, *Phil. Mag.* **10** (1964) 361.
16. S. MAHAJAN and G. Y. CHIN, *Acta Met.* **22** (1974) 1113.
17. H. -J. KESTENBACH, *Metallography* **10** (1977) 189.
18. K. RAJAN, ScD thesis, MIT, 1978.
19. K. H. G. ASHBEE, *Acta Met.* **15** (1967) 1129.
20. G. B. OLSON and M. COHEN, *Met. Trans. A* **7A** (1976) 1915.
21. J. A. VENABLES, in "Deformation Twinning", AIME Conference Series, Vol. 25 (Gordon and Breach, New York, 1964) p. 77.
22. A. H. COTTRELL and B. A. BILBY, *Phil. Mag.* **42** (1951) 573.
23. J. P. HIRTH, in "Deformation Twinning", AIME Conference Series, Vol. 25 (Gordon and Breach, New York, 1964) p. 112.
24. J. B. COHEN and J. WEERTMAN, *Acta Met.* **11** (1963) 997.
25. S. MAHAJAN and G. Y. CHIN, *ibid.* **21** (1973) 1353.
26. A. W. SLEESWYK, *Phil. Mag.* **8** (1963) 1467.
27. G. B. OLSON and M. COHEN, *Met. Trans. A* **7A** (1976) 1897.
28. R. D. HEIDENREICH and W. SHOCKLEY, Proceedings of the Conference on Strength of Solids (Bristol, 1947) p. 57.
29. G. B. OLSON and M. COHEN, *Met. Trans. A* **7A** (1976) 1905.
30. L. REMY, *Acta Met.* **26** (1978) 443.
31. L. REMY, *ibid.* **25** (1977) 711.
32. S. MAHAJAN, *Phys. Stat. Sol. A* **2** (1970) 189.
33. S. MAHAJAN and G. Y. CHIN, *Acta Met.* **21** (1973) 173.
34. K. S. RAGHAVAN, A. S. SASTRI and M. J. MARCINKOWSKI, *Trans. TMS-AIME* **245** (1969) 1569.
35. J. P. HIRTH and R. W. BALLUFFI, *Acta Met.* **21** (1973) 929.
36. S. MAHAJAN, D. E. BARRY and B. L. EYRE, *Phil. Mag.* **21** (1970) 43.

Received 17 June
and accepted 24 July 1981